Medicine & Science in Sports & Exercise Publish Ahead of Print

DOI: 10.1249/MSS.0000000000004120

Photobiomodulation Does Not Increase Mitochondrial Respiration in Skeletal Muscle or Skin Tissue in Humans

Thorben Aussieker[1,2], Heather L. Petrick[1], Lisa M.E. Kuin[1], Jeremias Kaiser[1], Cas J. Fuchs[1], Esther Kornips[1], Kostas Tsintzas[3], Scott Cooper[3], Sandra Lammers[4], Stephan Praet[5], Tim Snijders[1], and Luc J.C. van Loon[1]

[1]Department of Human Biology, NUTRIM, Institute for Nutrition and Translational Research in Metabolism, Maastricht University, Maastricht, THE NETHERLANDS; [2]Department of Health and Sport Sciences, TUM School of Medicine and Health, Technical University of Munich, GERMANY; [3]School of Life Sciences, University of Nottingham, Queen's Medical Centre, UNITED KINGDOM; [4]Revicura, Gastel, THE NETHERLANDS; [5]UCRISE, University of Canberra, Bruce, AUSTRALIA

Running Title: PHOTOBIOMODULATION, MUSCLE AND SKIN

Address for correspondence: L.J.C. van Loon, PhD., Department of Human Biology, Faculty of Health, Medicine and Life Sciences, Maastricht University, PO Box 616, 6200 MD Maastricht, The Netherlands; E-mail: l.vanloon@maastrichtuniversity.nl; Phone: +31-43-3881397; Fax: +31-43-3670976.

Conflict of Interest and Funding Source: L.J.C. vL. and his laboratory has received research grants, consulting fees, speaking honoraria, or a combination of these for research on the impact of exercise and nutrition on muscle metabolism. A full overview on research funding is provided at https://www.maastrichtuniversity.nl/l.vanloon.

ABSTRACT

Purpose: Low-level laser therapy, also referred to as photobiomodulation (PBM), is rapidly gaining popularity as a non-invasive treatment for various conditions and as a means to enhance health and performance. PBM has been proposed to directly increase mitochondrial activity in skin and skeletal muscle and activate various molecular signalling pathways. However, evidence for the proposed properties of PBM *in vivo* in humans is lacking.

Methods: In a within-participant study design, 12 healthy men and women (6/6 m/f; age: 25±6 y; BMI: 23.3±2.2 kg/m^2) received PBM on a randomized leg, while the other leg received sham-treatment (no light emitted, CON). Three cycles of PBM or sham-treatment were performed for 5 min 16 sec each (5.6 kJ light energy/cycle for PBM). Skin temperature was measured before and after treatment. After treatment, skin and muscle samples were collected from both legs. Mitochondrial respiration was measured in permeabilized muscle fibers and minced skin tissue using an Oroboros Oxygraph-O_2k. Muscle metabolic gene expression was assessed using custom made microfluidic cards.

Results: Skin temperature increased only in the PBM treated leg (+8.0±1.4 °C; P<0.001). No differences were observed between the PBM and CON treated legs in maximal complex I+II-linked respiration in skin (2.7±0.8 vs 2.6±0.7 *p*mol/sec/mg wet weight, respectively; P=0.66) or muscle (474±114 vs 467±81 *p*mol/sec/mg dry weight, respectively; P=0.71). Furthermore, no differences were observed in muscle mitochondrial ADP sensitivity (apparent ADP half-time: 1310±180 vs 1229±240 µM ADP, respectively; P=0.14). Of the 91 genes, expression between legs differed for 3 genes only.

Conclusions: A single session of photobiomodulation does not increase mitochondrial respiration in skin or underlying muscle tissue and does not modulate muscle gene expression *ex vivo* in humans.

Key Words: LOW-LEVEL LASER THERAPY (LLLT), PHOTOTHERAPY, MUSCLE, SKIN, MITOCHONDRIA

INTRODUCTION

Low-level laser therapy, now often referred to as photobiomodulation (PBM), is a non-invasive therapeutic modality that involves the application of low-power red or near-infrared light (600–1000 nm) to biological tissues. PBM is typically delivered via lasers or light-emitting diodes (LEDs) in the range of 5 to 500 mW and power density of 1 to 5 W/cm² (1). First experiments in the 1960s showed effects of PBM on hair growth and wound healing in mice (2, 3). Later, the same research group showed effects on non-healing skin ulcers in humans (4). Since the 1960s, the field of PBM has broadened and PBM is now frequently used as a treatment for a range of conditions including chronic pain (5-8) or oral mucositis (9, 10). PBM has been suggested to improve health by accelerating wound healing (11, 12), improving glucose control and insulin levels (13, 14) in animals. Furthermore, in humans, PBM has been shown to increase blood flow (15) and support functional capacity outcomes, such as the 6-min walk distance in COPD patients (16). Additionally, PBM has been suggested to increase fatigue resistance, endurance-type exercise performance, and recovery when combined with exercise in an acute setting in humans (17-20). Interestingly, longer term PBM treatment has been proposed to improve muscle performance and recovery (21, 22).

The reported impact of PBM is generally not attributed to thermal mechanisms, but its effects are thought to rely on photochemical processes, where light that is absorbed triggers a chemical transformation to induce its physiological effects at the cellular level (23). The laser produces red to near-infrared photons that are hypothesized to be absorbed by mitochondrial cytochrome c oxidase, enhancing electron transport, increasing the proton gradient, and stimulating ATP synthesis within mitochondria to support cellular metabolism (24-29). Additional proposed effects are increasing the production of reactive oxygen species, influencing

calcium metabolism, and facilitating tissue regeneration (12, 23, 30, 31). While most of these suggested effects are based on *in vitro* experiments, *in vivo* animal studies of PBM on skin have been reported to promote angiogenesis (32), increase signalling of anti-inflammatory proteins (33), increase collagen synthesis (34), and support wound healing (11, 12). Suggested effects on muscle tissue of animals include increased ATP synthesis (28) and upregulation of the expression of genes associated with the regulation of muscle mass (35).

The number of PubMed-indexed publications addressing photobiomodulation in the context of sport and exercise has been increasing substantially, from 44 articles in 2004 to 245 articles in 2024. Despite the increasing interest in the clinical and sports application of PBM (36), much of the mechanistic evidence for PBM-induced mitochondrial activation and molecular signalling is derived from *in vitro* and animal studies. So far, no work has been done to assess the proposed impact of PBM on skin or skeletal muscle tissue metabolism in humans. Therefore, we assessed the impact of PBM on mitochondrial respiration in both skin and muscle tissue and muscle gene expression *ex vivo* in humans. We included skin tissue because it represents the tissue directly exposed to PBM and is a clinically relevant target for PBM applications. Assessing both skin and underlying muscle allowed us to evaluate whether any acute effects were confined to the direct light exposure or whether they indeed can extend deeper into skeletal muscle tissue. We hypothesized that PBM activates both muscle and skin tissue by stimulating mitochondrial respiration and upregulating skeletal muscle gene expression. We recruited 12 healthy young, recreationally active men and women to receive PBM applied to one randomly chosen leg, while the other leg received a sham treatment. Muscle and skin tissue samples were collected after treatment to assess mitochondrial respiration and muscle metabolic gene expression.

METHODS

Participants

A total of 12 healthy, recreationally active men (*n*=6) and women (*n*=6) volunteered to participate in this within-participant clinical trial. Participants were 25±6 years old, had a body mass of 70.9±15.1 kg, were 1.74±0.12 m tall, had a BMI of 23.3±2.2 kg/m², and had a mean Fitzpatrick skin type of 2.4±1.0. After pretesting, one randomly chosen leg of the participants received PBM, while the other leg received sham treatment (no light emitted, CON). All participants were informed of the nature and possible risks of the experimental procedures before their written informed consent was obtained. This study was approved by the Medical Ethical Committee of the Maastricht University Medical Centre and conforms to the principles outlined in the declaration of Helsinki as revised in October 2024 for use of human participants and tissue. The trial was registered at ClinicalTrials.gov (NCT06330363) and was conducted between June and November 2024 at Maastricht University, Maastricht, The Netherlands. Clinical Trial Center Maastricht independently monitored the study.

Pretesting

Participants (aged 18–35 y with a BMI >18.5 and <30.0 kg/m²; performed ≤4 hours of exercise per week) underwent an initial screening session to assess height, body mass, and study eligibility. Participants were deemed healthy based on their responses to a medical questionnaire and were excluded from participation when smoking, using medication that affected tissue metabolism, having any musculoskeletal and/or skin diseases, participating in a structured exercise program, being or planning to be pregnant.

Diet and physical activity

All participants refrained from strenuous physical activity and alcohol consumption and filled out food intake and physical activity questionnaires for 2 days prior to the experimental trial. Participants consumed the same standardized meal before 21:00 PM on the evening before the experimental trial. This prepackaged standardized meal provided 1.71 MJ, with 55% of the energy from carbohydrate, 30% energy from fat, and 15% energy from protein. Thereafter, participants remained fasted until the experimental test day.

Experimental protocol

For a schematic representation of the experimental test day, see Figure 1. In the morning of the experimental test day (starting between 8:00 and 9:00 AM) participants arrived at the laboratory by public transport in an overnight fasted state and were assigned to a bed. The Fitzpatrick system was used to assess their skin type (37). The treatment areas of both legs were marked and shaved. The anatomical location was on the lateral aspect of the upper leg, over the *M. vastus lateralis*, exactly one-third of the distance between the patella and the greater trochanter. Participants rested in a supine position for 30 min. Afterwards skin temperature of both legs was assessed in the middle of the treatment area, as well as on top of the upper thigh as a reference point, by a digital infrared thermometer (Onbo Electronics Co. Ltd., China). Thereafter, the PBM or CON treatment started in a randomized order (stratified for sex, http://www.randomization.com/). Immediately after succession of the last set of each treatment, skin temperature was assessed at the same areas as done before the treatment. Biopsies from both legs were taken in randomized order. For each leg, the muscle biopsies were collected first, followed by the skin biopsies. All biopsies were performed by the same physician. The time between finishing the PBM/CON treatment and collection of the tissue samples of the associated

leg was noted. Researchers performing muscle and skin analysis were blinded to the treatment of the legs.

Photobiomodulation treatment

PBM was performed using a Cube plus30 (Eltech K-Laser s.r.l., Italy) with the K-Laser Cube Extend Plus extension to apply the laser energy uniformly on an area with a diameter of 100 mm. Settings were based on manufacturer's guidelines for skin and deep tissue stimulation. PBM was performed 3 times for 5 min 16 sec of treatment separated by 5 min of rest. During the rest period, or before the first set of PBM, depending on the randomization of treatment order, the sham treatment was performed (CON). The sham treatment consisted of the same setup of the laser device hand piece, with no energy/light emitted while the laser device was making the same sounds (placebo mode). In total 16.8 kJ in form of light energy was applied (3 x 5.6 kJ) in PBM. All 4 available wavelengths were used (660, 800, 905 and 970 nm) in intermittent Continuous Wave (CW), Pulsed Wave (PW), SuperPulse (SP), and IntenseSuperPulse (ISP) mode. During the treatment period protective goggles (K-Laser Protective Goggles, Eltech K-Laser s.r.l.) were worn. PBM was applied by trained and certified personnel.

Muscle and skin tissue sampling

Muscle biopsy samples were collected using a 5 mm Bergström needle custom-adapted for manual suction. Samples were obtained from the middle region of the *M. vastus lateralis*, ~3 cm below entry through the fascia located behind the area where the treatment was applied, under 2% xylocaine local anesthesia. Muscle samples were freed from any visible non-muscle material. A small portion of muscle (~15 mg) was sectioned and immediately placed into ice-cold BIOPS preservation buffer (50 mM MES, 7.23 mM K_2EGTA, 2.77 mM CaK_2EGTA, 20 mM imidazole, 0.5 mM dithiothreitol, 20 mM taurine, 6.56 mM $MgCl_2 6H_2O$, 5.77 mM Na_2ATP,

15 mM Na_2PCr; pH 7.1) for mitochondrial respiration experiments as previously described (38). The remaining muscle tissue (~100 mg) was immediately frozen in liquid nitrogen and stored at −80°C until further processing. Skin biopsies samples were obtained from the thigh in the middle of the treatment area by the punch biopsy technique as described by Zuber (39) using a 4 mm punch biopsy instrument (KAI Medical, Solingen, Germany) under 2% xylocaine local anesthesia. The skin was penetrated by the skin punch biopsy instrument until the subcutaneous fat was reached. The skin layers were lifted, and the skin was cut free from subcutaneous tissues using scissors. For each leg, two skin punches were taken and were freed from any visible non-skin material. One skin sample was immediately placed in 1 mL of ice-cold BIOPS preservation buffer for mitochondrial respiration experiments. The other one was immediately frozen in liquid nitrogen and stored at −80°C until further processing.

Mitochondrial respiration analysis

For skeletal muscle mitochondrial respiration experiments, muscle tissue was trimmed of any fat and connective tissue under a microscope and separated into bundles using fine-tipped forceps (38). Fiber bundles were permeabilized with 40 µg/mL saponin in 1.5 mL BIOPS for 30 min while continuously rotating at 4˚C. Subsequently, fiber bundles were transferred to 1.5 mL MiR05 respiration buffer (0.5 mM EGTA, 3 mM $MgCl_26H_2O$, 60 mM potassium lactobionate, 10 mM KH_2PO_4, 20 mM HEPES, 110 mM sucrose, 1 g/L fatty acid free bovine serum albumin; pH 7.1) and washed for 15 min. Mitochondrial respiration experiments were then performed in duplicate at 37˚C in 2 mL of MiR05 with constant stirring at 750 rpm, in an Oroboros Oxygraph-2k (Oroboros Instruments, Innsbruck, Austria). Experiments were performed in the presence of 5 µM blebbistatin. First, 5 mM pyruvate (P) and 1 mM malate (M) were added to assess leak respiration. Various concentrations of ADP (D) were then titrated (25, 100, 175, 250, 500, 1000,

2000, 4000, 6000, 8000, 10000, 12000 µM ADP). 10 mM glutamate (G, maximal complex I-linked respiration), 10 mM succinate (S, maximal complex I+II-linked respiration) and 10 µM cytochrome C (C, to assess membrane integrity) were sequentially added. Any experiment in which cytochrome C increased respiration by more than 10% was excluded from analysis. Respiratory control ratios (RCR) were calculated as: maximal ADP-supported respiration (presence of ADP; PMD) / pyruvate+malate-supported respiration (absence of ADP; PM). All fiber bundles were recovered, freeze-dried, weighed, and respiration data were normalized to fiber dry weight. Mitochondrial ADP kinetics were analyzed using constrained one-phase associations (Y0 = 0 and plateau = 100) to determine the apparent half-time using GraphPad Prism 10.0 Software.

Skin mitochondrial respiration experiments were performed based on methodologies previously used for assessing adipose tissue mitochondrial respiration (40, 41). Skin tissue was minced in ice-cold BIOPS using scissors and transferred to 1 mL of ice-cold MiR05 respiration buffer. Then, skin tissue was blotted dry on filter paper, weighed (~15 mg wet weight), and transferred to an Oroboros Oxygraph-2k for measurement of mitochondrial respiration. Experiments were performed in singlicate at 37˚C in 2 mL of MiR05 with constant stirring at 750 rpm. First, 50 µg/mL saponin, 5 mM pyruvate, and 2 mM malate were added. Sequential additions of 5 mM ADP, 10 mM glutamate, 10 mM succinate, and 10 µM cytochrome C were performed. Any experiment in which cytochrome C increased respiration by more than 10% was excluded from analysis. All skin respiration data were normalized to tissue wet weight measured prior to experiments.

Gene expression analysis

RNA was extracted using TRIzol™ (ThermoFisher Scientific, MA, USA) from 15-20 mg of frozen muscle tissue by the method of Chomczynski and Sacchi (42) and quantified using a NanoDrop One spectrophotometer (ThermoFisher Scientific). All samples had A260/A280 values between 1.9 and 2.1. The cDNA synthesis was performed using Invitrogen SuperScript™ in accordance with manufacturer's guidelines. Real time PCR (qPCR) was performed using custom Taqman® Low Density Microfluidic cards (ABI) on a 7900HT Fast Real-Time PCR System (ABI Applied Biosystems), as previously described (43). Relative quantification of expression of genes of interest (listed in Supplemental Table 1, Supplemental Digital Content, https://links.lww.com/MSS/D462) was performed using the geometric mean of housekeeping genes alpha actin (*ACTA1*), hydroxymethylbilane synthase (*HMBS*) and 18S ribosomal RNA (*18S*) as endogenous control. The comparative threshold cycle (Ct) method was used to process the data where ΔCt=Ct target gene – Ct endogenous control (geometric mean of *HMBS, ACTA1, 18S*). Data were then normalized to an internal calibrator sample (ΔΔCt), and relative quantification (RQ) values were obtained using the equation $2^{-\Delta\Delta Ct}$. Two genes (*IL-10* and *TERT*) were undetectable and therefore data for 91 genes are presented.

Statistical analysis

An *a priori* sample size calculation was performed using the primary outcome, maximal muscle mitochondrial respiration (PMDGS). Based on yet unpublished mitochondrial respiration data from our research group (preliminary data) looking at the effects of acute running exercise on mitochondrial respiration in men and women (6 each), we calculated an effect size of 0.92 (using the means and SD of pre and post running values and presented as groups 1 and 2, respectively) and a correlation between groups of 0.57 (groups is referring to the pre and post

exercise values of the full group). A sample size of 12 was calculated for a paired sample t-test (PBM vs CON) with a power of 80% (1-β = 0.8), and a significance level of 5% (α = 0.05). Skin temperature data were analyzed by repeated measures ANOVA with time (pre/post) and treatment (PBM/CON) as within-participants factors. In case of a significant interaction effect, individual time points were analyzed using paired sample t-tests. Data of mitochondrial respiration and gene expression were compared between treatments (PBM vs CON) using paired samples t-tests. No correction for multiple comparisons was applied to the exploratory gene expression analysis. Statistical significance was set at $P<0.05$. All data in text are expressed as mean±SD. Calculations were performed using SPSS 29.0 (SPSS Inc., Chicago, IL) and GraphPad Prism 10.0 (GraphPad Software, Boston, MA).

RESULTS

Time of sample collection and skin temperature

Muscle samples of the PBM and CON leg were collected 28±7 and 29±7 min after completion of the last set of each treatment, respectively (P=0.77). Skin samples of the PBM and CON leg were collected 33±6 and 34±9 min after succession of the last set of each treatment, respectively (P=0.75). Skin temperature of the reference area at the upper thigh did not change over time (PBM leg: Pre 31.2±1.3 vs Post 31.1±2.3 °C, P=0.87; CON leg: Pre 30.7±1.7 vs Post 30.3±1.3 °C, P=0.45). A significant time x treatment interaction was observed for skin temperature of the treatment areas (P<0.001, Figure 2). Skin temperature of the treatment area increased by 8.0±1.4 °C in PBM (Pre 31.3±1.4 vs Post 39.3±0.7 °C, P<0.001) and remained unchanged in the CON leg (Pre 31.1±1.2 vs Post 30.6±0.8 °C, P=0.36, Figure 2).

Skin mitochondrial respiration

In skin tissue, leak mitochondrial respiration (PM, pyruvate+malate), maximal ADP-supported respiration (+ADP, PMD), and maximal complex I-linked respiration (+glutamate, PMDG) did not differ between PBM and CON (all P>0.66, Figure 3). Furthermore, maximal complex I+II-linked respiration (+succinate, PMDGS) was not different (2.7±0.8 vs 2.6±0.7 *p*mol/sec/mg wet weight in PBM vs CON, respectively; P=0.66, Figure 3). The ability of ADP to stimulate respiration (respiratory control ratio, RCR) did not differ between the two treatments (Figure 3).

Muscle mitochondrial respiration

In permeabilized muscle fibers, leak mitochondrial respiration (PM), maximal ADP-supported respiration (+ADP, PMD), and maximal complex I-linked respiration (+glutamate, PMDG) were not altered by PBM (all P>0.37, Figure 4A). In addition, maximal complex I+II-linked respiration (+succinate, PMDGS) did not differ between legs (474±114 vs 467±81 *p*mol/sec/mg dry weight in PBM vs CON, respectively; P=0.71, Figure 4A). The ability of ADP to stimulate respiration (RCR) was not different between PBM and CON (Figure 4A). Submaximal mitochondrial respiration was not different in response to any concentration of ADP tested (25 – 10,000 µM, Figure 4B). In addition, no differences were observed in mitochondrial sensitivity to ADP (apparent ADP half-time: 1310±180 vs 1229±240 µM ADP in PBM vs CON, respectively; P=0.14, Figure 4B inset).

Muscle gene expression

Of 91 measured genes, only 3 genes were differently affected between muscle samples from the PBM and CON leg. There were no differences in genes related to mitochondrial tricarboxylic acid (TCA) cycle (Figure 5A, B), mitochondrial respiration (Figure 5C, D), or

carbohydrate metabolism (Figure 5E, F). Two genes involved in fatty acid metabolism were altered by PBM (Figure 5G, H), whereby PBM resulted in higher values of ACAT1 (1.91±0.33 vs 1.77±0.38 in PBM vs CON, respectively; P=0.01) and LPL (2.44±1.04 vs 2.02±0.67 in PBM vs CON, respectively; P=0.04). There were no differences in genes involved in oxidative stress (Figure 6A, B), inflammation (Figure 6C, D), cell proliferation and differentiation (Figure 6E, F), or heat shock proteins (Figure 6G, H). However, values for the endoplasmic reticulum stress gene DAPK1 were lower in PBM (2.08±0.76 vs 2.62±1.04 in PBM vs CON, respectively; P=0.03; Figure 6I, J). For all other measured genes, no differences between the legs were detected (P values between 0.064-0.95; Supplemental Figure 1, Supplemental Digital Content, https://links.lww.com/MSS/D462).

DISCUSSION

In the present study, an acute PBM treatment increased skin temperature with no changes in skin mitochondrial respiration. Furthermore, photobiomodulation did not affect submaximal or maximal mitochondrial respiration in underlying skeletal muscle tissue. The absence of differences in muscle mitochondrial respiration were mirrored by the lack of differences in nearly all muscle metabolic gene expression patterns in the PBM treated leg.

The PBM protocol used in this study delivered a substantial amount of energy (16.8 kJ) across multiple wavelengths (660, 800, 905 and 970 nm) and operating modes, reflecting one of the most comprehensive energy-transfer approaches currently available. This intense protocol effectively elevated skin temperature by ~8 °C (Figure 2), demonstrating that considerable energy reached the tissue surface despite PBM generally being considered a non-thermal therapy (23-29). The observed increase in skin temperature was comparable to that seen with 40 min of infrared sauna exposure (44) but remained lower than the elevation in skin temperature that is

observed following a string (local) hot-water immersion protocol (45). Although increased skin temperature suggests that underlying muscle may have warmed modestly (45), the extent of deeper tissue heating remains unclear. As it is not possible to directly quantify tissue dosimetry or light fluence at the depth of the muscle biopsy collection, we can only speculate on the light energy penetration deep into skeletal muscle tissue. Transmission of red and near-infrared light through biological tissues is strongly wavelength- and tissue-dependent, with *ex vivo* studies showing that 800–905 nm light penetrates deeper than 970 nm light, but that >90% of near-infrared laser energy may still be absorbed within the first 10 mm of tissue (46). In line with this, transmission studies using 660, 830, and 904 nm light show a progressive reduction in transmitted power with increasing tissue thickness (47) and human skin measurements at 850 nm have demonstrated marked attenuation within superficial tissue layers (48). Therefore, although the increase in skin temperature confirms energy delivery to the tissue surface, we can only speculate whether sufficient light energy could have reached the depth of the muscle tissue sampled. Nevertheless, the pronounced surface heating indicates that the applied high energy PBM protocol induced a clear local tissue response, suggesting a possibility for physiological responses if PBM had been proven effective to stimulate skin and/or muscle metabolism.

PBM has been proposed to influence cellular metabolism through photochemical mechanisms, independent of heat, with mitochondrial activation typically cited as the downstream effect (24-29). Mitochondrial respiration is widely used as a proxy for metabolic function (49, 50), yet *ex vivo* assessments in human skin are rare and largely limited to cell culture work in fibroblasts (51, 52). In the current study, we collected skin tissue samples from both the treated and untreated leg. Skin tissue samples from the CON leg demonstrated the expected increases in mitochondrial respiration rates in response to additions of pyruvate and

malate, saturating concentrations of ADP, glutamate (maximal complex I) and succinate (maximal complex II, Figure 3). However, maximal mitochondrial respiration rates of skin tissue were ~150-fold lower than those observed in skeletal muscle tissue (Figures 3 and 4, (53, 54)). This is in line with the proposed lower mitochondrial density of skin, although there are no data directly comparing skin and muscle tissue mitochondrial contents. Importantly, we used all layers of skin in the present study. Despite the substantial elevation in skin temperature, PBM did not modulate mitochondrial respiration in skin tissue. We observed identical patterns of mitochondrial respiration in the PBM-treated and CON leg in all substrate conditions (Figure 3). These findings suggest that neither the delivered light nor the accompanied thermal response were able to stimulate mitochondrial metabolism in healthy skin tissue. However, PBM has been shown to have some clinical efficacy in treating conditions such as oral mucositis (55, 56). Of course, the oral epithelium is both anatomically and structurally much different from skin, and may be more prone to the proposed impact of PBM. Furthermore, it can be speculated that the oral epithelium is only responsive to PBM under pathological conditions of increased inflammation. Nonetheless, our results clearly indicate that acute PBM treatment does not impact mitochondrial respiration in healthy human skin.

We also examined whether PBM affected mitochondrial respiration in skeletal muscle. Given the proximity of muscle to the treatment site, PBM could theoretically influence muscle metabolism via direct photon penetration or indirect heating. The muscle samples collected from the CON leg displayed normal substrate-driven increases in respiration (Figure 4, (53, 54)). Similar to skin tissue data, PBM exposure did not result in changes in maximal mitochondrial respiration in skeletal muscle (Figure 4). In addition, submaximal mitochondrial respiration and mitochondrial ADP sensitivity between muscle samples collected from the treated and sham-

treated leg showed no differences. Altogether, this provides evidence that PBM is not able to acutely modulate mitochondrial respiration *ex vivo* in skeletal muscle tissue.

To further explore the potential impact of PBM on the activation or downregulation of metabolic pathways in skeletal muscle tissue, we also assessed muscle gene expression across a large collection of 91 genes representing pathways that may be involved in the proposed PBM-mediated effects. The latter include genes involved in regulating mitochondrial metabolism, oxidative stress, inflammation, and cellular remodeling. While *in vitro* (12, 23, 30, 31) as well as *in vivo* animal (28, 32, 33, 35) studies have frequently reported rapid upregulation of metabolic genes following PBM exposure, we observed no meaningful changes in skeletal muscle gene expression (Figures 5 and 6). Only three genes differed between legs, namely ACAT1 and LPL involved in fatty acid metabolism as well as DAPK1 involved in endoplasmic reticulum stress regulation. As these gene expression analyses were not corrected for multiple comparisons, these three nominal differences should be interpreted with caution and may likely reflect false-positive findings, which is consistent with the absence of coordinated changes across any major biological pathway. Together, the absence of any overt transcriptional response aligns with the lack of metabolic mitochondrial effects and underscores our findings that acute PBM does not seem to activate molecular signaling pathways in muscle tissue of healthy adults.

PBM continues to gain popularity as a non-invasive therapeutic modality in both clinical practice and athletic sports settings. However, the present findings do not support the proposed mechanisms by which PBM is thought to enhance tissue health or performance in healthy individuals. Although the clinical evidence supporting PBM for treating oral mucositis is strong (55, 56), the broader literature remains mixed, and findings across tissues and conditions are inconsistent (57). In the athletic context, acute photobiomodulation therapy performed using

LEDs was not successful in increasing running performance (58). It remains possible that repeated PBM sessions, rather than a single exposure, are necessary to induce measurable changes in muscle or skin. Nevertheless, *in vitro* studies suggest that PBM should exert immediate effects at the cellular level, raising questions about the magnitude of PBM's biological impact *in vivo*. While our results make us cautious regarding claims of acute metabolic activation in healthy tissues, they also underscore the need for rigorous mechanistic studies that evaluate the proposed impact of PBM under more clinically or physiologically stressed conditions.

Our findings should also be interpreted in the context of the highly heterogeneous PBM literature. Studies reporting beneficial effects often differ substantially with respect to light source, wavelength, dose, treatment timing, repetition of treatment, and the selected outcome measures. We have used all available wave length and modes, providing a high dosage of light energy to maximize the potential to induce any physiological or biological responses. In addition, many human studies have focused on functional outcomes such as fatigue resistance, endurance performance, or recovery, whereas we assessed direct tissue-level outcomes in healthy, resting, recreationally active participants after a single exposure. Therefore, our data do not exclude the possibility that PBM may exert context-dependent effects under repeated application, in conjunction with exercise, or in tissues under greater physiological or pathological stress. A few limitations should be acknowledged. First, our contralateral-leg sham design allowed us to minimize inter-individual variability and reduce the biopsy burden, but it did not include a completely untreated control condition. Therefore, we cannot fully exclude device handling-related effects, placebo-related cues, or possible systemic/bilateral responses that may have attenuated between-leg differences. Second, tissue sampling was performed ~30 min on

average after treatment, which is appropriate to assess immediate metabolic effects, but may have been too early to detect more delayed transcriptional responses of PBM. Third, the present study was performed in healthy, recreationally active young adults, and responses may differ in less fit individuals or under clinically relevant conditions characterized by injury, inflammation, and/or metabolic dysfunction.

CONCLUSIONS

In conclusion, a single session of photobiomodulation does not modulate mitochondrial respiration in skin or muscle tissue or induce substantial changes in skeletal muscle gene expression in humans. It remains to be established whether more prolonged application of photobiomodulation over days, weeks, or months may be effective to induce measurable metabolic effects and, as such, promote tissue repair and regeneration *in vivo* in humans.

Acknowledgements

The authors express their gratitude to all study participants for their time and commitment. We acknowledge Eltech K-Laser s.r.l. for lending us the laser device for this research study at no cost. L.J.C. vL. and his laboratory has received research grants, consulting fees, speaking honoraria, or a combination of these for research on the impact of exercise and nutrition on muscle metabolism. A full overview on research funding is provided at https://www.maastrichtuniversity.nl/l.vanloon. T.A., H.L.P., L.M.E.K., J.K., C.J.F., E.K., K.T., S.C., S.L., S.P. and T.S. report no conflicts of interest related to this work. The results of the study are presented clearly, honestly, and without fabrication, falsification, or inappropriate data manipulation. The results of the present study do not constitute endorsement by the American College of Sports Medicine. This trial was registered at ClinicalTrials.gov (NCT06330363).

REFERENCES

1. Posten W, Wrone DA, Dover JS. et al. Low-level laser therapy for wound healing: mechanism and efficacy. *Dermatol Surg*. 2005;31(3):334-40.
2. Mester E, Ludany G, Selyei M, Szende B. *The stimulating effect of low power laser rays on biological systems*. Medical Univ., Budapest1968. Available from: Medical Univ., Budapest.
3. Mester E, Szende B, Tota J. Effect of laser on hair growth of mice. *Kiserl Orvostud*. 1967;19(7):628.
4. Mester E, Mester AF, Mester A. The biomedical effects of laser application. *Lasers Surg Med*. 1985;5(1):31-9.
5. Glazov G, Yelland M, Emery J. Low-level laser therapy for chronic non-specific low back pain: a meta-analysis of randomised controlled trials. *Acupunct Med*. 2016;34(5):328-41.
6. Chow RT, Johnson MI, Lopes-Martins RAB, Bjordal JM. Efficacy of low-level laser therapy in the management of neck pain: a systematic review and meta-analysis of randomised placebo or active-treatment controlled trials. *Lancet*. 2009;374(9705):1897-908.
7. Maia MLdM, Bonjardim LR, Quintans JdSS, et al. Effect of low-level laser therapy on pain levels in patients with temporomandibular disorders: a systematic review. *J Appl Oral Sci*. 2012;20:594-602.
8. Qaseem A, Wilt TJ, McLean RM, et al. Noninvasive treatments for acute, subacute, and chronic low back pain: a clinical practice guideline from the American College of Physicians. *Ann Intern Med*. 2017;166(7):514-30.

9. Zadik Y, Arany PR, Fregnani ER, et al. Systematic review of photobiomodulation for the management of oral mucositis in cancer patients and clinical practice guidelines. *Support Care Cancer*. 2019;27(10):3969-83.

10. Antunes HS, Herchenhorn D, Small IA, et al. Long-term survival of a randomized phase III trial of head and neck cancer patients receiving concurrent chemoradiation therapy with or without low-level laser therapy (LLLT) to prevent oral mucositis. *Oral Oncol*. 2017;71:11-5.

11. Kovács, Iren B, Mester E, Görög P. Stimulation of wound healing with laser beam in the rat. *Experientia*. 1974;30(11):1275-6.

12. Yang WZ, Chen JY, Yu JT, Zhou LW. Effects of low power laser irradiation on intracellular calcium and histamine release in RBL-2H3 mast cells. *Photochem Photobiol*. 2007;83(4):979-84.

13. Castro KMR, de Paiva Carvalho RL, Junior GMR, et al. Can photobiomodulation therapy (PBMT) control blood glucose levels and alter muscle glycogen synthesis? *J Photochem Photobiol B*. 2020;207:111877.

14. de Castro Magalhães F, Ferraresi C. Photobiomodulation therapy on the treatment of insulin resistance: a narrative review. *Photobiomodul Photomed Laser Surg*. 2022;40(9):597-603.

15. Heu F, Forster C, Namer B, Dragu A, Lang W. Effect of low-level laser therapy on blood flow and oxygen-hemoglobin saturation of the foot skin in healthy subjects: a pilot study. *Laser Ther*. 2013;22(1):21-30.

16. de Souza GHM, Ferraresi C, Moreno MA, et al. Acute effects of photobiomodulation therapy applied to respiratory muscles of chronic obstructive pulmonary disease patients:

a double-blind, randomized, placebo-controlled crossover trial. *Lasers Med Sci*. 2020;35(5):1055-63.

17. de Almeida P, Lopes-Martins RÁB, De Marchi T, et al. Red (660 nm) and infrared (830 nm) low-level laser therapy in skeletal muscle fatigue in humans: what is better? *Lasers Med Sci*. 2012;27:453-8.

18. De Marchi T, Leal Junior ECP, Bortoli C, et al. Low-level laser therapy (LLLT) in human progressive-intensity running: effects on exercise performance, skeletal muscle status, and oxidative stress. *Lasers Med Sci*. 2012;27:231-6.

19. Leal ECP, Lopes-Martins RÁB, Frigo L et al. Effects of low-level laser therapy (LLLT) in the development of exercise-induced skeletal muscle fatigue and changes in biochemical markers related to postexercise recovery. *J Orthop Sports Phys Ther*. 2010;40(8):524-32.

20. Leal Junior ECP, Lopes-Martins RÁB, Vanin AA, et al. Effect of 830 nm low-level laser therapy in exercise-induced skeletal muscle fatigue in humans. *Lasers Med Sci*. 2009;24:425-31.

21. Ferraresi C, de Brito Oliveira T, de Oliveira Zafalon L, et al. Effects of low level laser therapy (808 nm) on physical strength training in humans. *Lasers Med Sci*. 2011;26:349-58.

22. de Brito Vieira WH, Ferraresi C, de Andrade Perez SE, Baldissera V, Parizotto NA. Effects of low-level laser therapy (808 nm) on isokinetic muscle performance of young women submitted to endurance training: a randomized controlled clinical trial. *Lasers Med Sci*. 2012;27:497-504.

23. Huang YY, Chen AC, Carroll JD, Hamblin MR. Biphasic dose response in low level light therapy. *Dose Response*. 2009;7(4):358-83.

24. de Souza da Fonseca A, de Souza Alves E, de Paoli F, Mencalha AL. Low-power therapeutic lasers on mRNA levels. *Lasers Med Sci*. 2022;37(5):2353-62.

25. Zecha JA, Raber-Durlacher JE, Nair RG, et al. Low level laser therapy/photobiomodulation in the management of side effects of chemoradiation therapy in head and neck cancer: part 1: mechanisms of action, dosimetric, and safety considerations. *Support Care Cancer*. 2016;24(6):2781-92.

26. Trajano LAdSN, Siqueira PB, Rodrigues MMdS, et al. Does photobiomodulation alter mitochondrial dynamics? *Photochem Photobiol*. 2025;101(1):21-37.

27. Passarella S, Ostuni A, Atlante A, Quagliariello E. Increase in the ADP/ATP exchange in rat liver mitochondria irradiated in vitro by helium-neon laser. *Biochem Biophys Res Commun*. 1988;156(2):978-86.

28. Silveira PC, da Silva LA, Fraga DB et al. Evaluation of mitochondrial respiratory chain activity in muscle healing by low-level laser therapy. *J Photochem Photobiol B.* 2009;95(2):89-92.

29. Maghfour J, Ozog DM, Mineroff J, et al. Photobiomodulation CME part I: overview and mechanism of action. *J Am Acad Dermatol*. 2024;91(5):793-802.

30. de Freitas LF, Hamblin MR. Proposed mechanisms of photobiomodulation or low-level light therapy. *IEEE J Sel Top Quantum Electron*. 2016;22(3):7000417.

31. Rupel K, Zupin L, Colliva A, et al. Photobiomodulation at multiple wavelengths differentially modulates oxidative stress in vitro and in vivo. *Oxidative Med Cell Longev.* 2018;2018:6510159.

32. Cury V, Moretti AIS, Assis L, et al. Low level laser therapy increases angiogenesis in a model of ischemic skin flap in rats mediated by VEGF, HIF-1α and MMP-2. *J Photochem Photobiol B.* 2013;125:164-70.

33. De Lima FM, Albertini R, Dantas Y, et al. Low-level laser therapy restores the oxidative stress balance in acute lung injury induced by gut ischemia and reperfusion. *Photochem Photobiol*. 2013;89(1):179-88.

34. Dang Y, Liu B, Liu L et al. The 800-nm diode laser irradiation induces skin collagen synthesis by stimulating TGF-β/Smad signaling pathway. *Lasers Med Sci*. 2011;26:837-43.

35. Macedo MM, Mafra FFP, Teixeira CdB, et al. Photobiomodulation therapy modulates muscle gene expression and improves performance of rats subjected to a chronic resistance exercise protocol. *Photobiomodul Photomed Laser Surg*. 2020;38(12):713-9.

36. Lawrence J, Sorra K. Photobiomodulation as medicine: low-level laser therapy (LLLT) for acute tissue injury or sport performance recovery. *J Funct Morphol Kinesiol*. 2024;9(4):181.

37. Fitzpatrick TB. The validity and practicality of sun-reactive skin types I through VI. *Arch Dermatol*. 1988;124(6):869-71.

38. Pinckaers PJM, Petrick HL, Horstman AMH, et al. Oleuropein supplementation increases resting skeletal muscle fractional pyruvate dehydrogenase activity but does not influence whole-body metabolism: a randomized, double-blind, and placebo-controlled trial in healthy, older males. *J Nutr*. 2025;155(5):1373-86.

39. Zuber TJ. Punch biopsy of the skin. *Am Fam Phys*. 2002;65(6):1155-8.

40. Petrick HL, Ogilvie LM, Brunetta HS, et al. Dietary nitrate and corresponding gut microbiota prevent cardiac dysfunction in obese mice. *Diabetes*. 2023;72(7):844-56.

41. Politis-Barber V, Brunetta HS, Paglialunga S, Petrick HL, Holloway GP. Long-term, high-fat feeding exacerbates short-term increases in adipose mitochondrial reactive oxygen species, without impairing mitochondrial respiration. *Am J Physiol Endocrinol Metab*. 2020;319(2):E376-87.

42. Chomczynski P, Sacchi N. Single-step method of RNA isolation by acid guanidinium thiocyanate-phenol-chloroform extraction. *Anal Biochem*. 1987;162(1):156-9.

43. Tsintzas K, Norton L, Chokkalingam K, et al. Independent and combined effects of acute physiological hyperglycaemia and hyperinsulinaemia on metabolic gene expression in human skeletal muscle. *Clin Sci*. 2013;124(11):675-86.

44. Schenaarts L, Hendriks FK, Fuchs CJ, et al. A single sauna session does not improve postprandial blood glucose handling in individuals with type 2 diabetes mellitus: a cross-over, randomized, controlled trial. *Exp Clin Endocrinol Diabetes*. 2024;132(11):622-30.

45. Fuchs CJ, Smeets JS, Senden JM, et al. Hot-water immersion does not increase postprandial muscle protein synthesis rates during recovery from resistance-type exercise in healthy, young males. *J Appl Physiol*. 2020;128(4):1012-22.

46. Kaub L, Schmitz C. More than ninety percent of the light energy emitted by near-infrared laser therapy devices used to treat musculoskeletal disorders is absorbed within the first ten millimeters of biological tissue. *Biomedicines*. 2022;10(12):3204.

47. Barbosa RI, de Oliveira Guirro EC, Bachmann L, Brandino HE, de Jesus Guirro RR. Analysis of low-level laser transmission at wavelengths 660, 830 and 904 nm in biological tissue samples. *J Photochem Photobiol B*. 2020;209:111914.

48. Esnouf A, Wright PA, Moore JC, Ahmed S. Depth of penetration of an 850nm wavelength low level laser in human skin. *Acupunct Electrother Res.* 2007;32(1-2):81-6.

49. Divakaruni AS, Jastroch M. A practical guide for the analysis, standardization and interpretation of oxygen consumption measurements. *Nat Metab*. 2022;4(8):978-94.

50. Sharma E, Fotooh Abadi L, Kombe Kombe JA, et al. Overview of methods that determine mitochondrial function in human disease. *Metabolism*. 2025;170:156300.

51. Haylett W, Swart C, Van der Westhuizen F, et al. Altered mitochondrial respiration and other features of mitochondrial function in parkin-mutant fibroblasts from Parkinson's disease patients. *Parkinsons Dis*. 2016;2016(1):1819209.

52. Sreedhar A, Aguilera-Aguirre L, Singh KK. Mitochondria in skin health, aging, and disease. *Cell Death Dis*. 2020;11(6):444.

53. Fuchs CJ, Betz MW, Petrick HL, et al. Repeated passive heat treatment increases muscle tissue capillarization, but does not affect postprandial muscle protein synthesis rates in healthy older adults. *J Physiol*. 2025;603(1):167-86.

54. Petrick HL, Pignanelli C, Barbeau PA, et al. Blood flow restricted resistance exercise and reductions in oxygen tension attenuate mitochondrial H2O2 emission rates in human skeletal muscle. *J Physiol*. 2019;597(15):3985-97.

55. Zadik Y, Arany PR, Fregnani ER, et al. Systematic review of photobiomodulation for the management of oral mucositis in cancer patients and clinical practice guidelines. *Support Care Cancer*. 2019;27(10):3969-83.

56. Parra-Rojas S, Cassol Spanemberg J, del Mar Díaz-Robayna N, Peralta-Mamani M, Velázquez Cayón RT. Assessing the cost-effectiveness of photobiomodulation for oral

mucositis prevention and treatment: a systematic review. *Biomedicines*. 2024;12(10):2366.

57. Son Y, Lee H, Yu S, et al. Effects of photobiomodulation on multiple health outcomes: an umbrella review of randomized clinical trials. *Syst Rev*. 2025;14(1):160.

58. do Nascimento AP, de Oliveira GA, Bressanin JPB, et al. Acute dose-response effect of photobiomodulation therapy on 5-km running performance in trained runners: a randomized, double-blind, placebo-controlled, crossover study. *Lasers Med Sci*. 2024;39(1):145.**FIGURE LEGENDS**

Figure 1. Schematic representation of the experimental testing day.

Figure 2. Skin temperature before and after photobiomodulation and control treatment in healthy, young adults (*n*=12). Bars represent means with circles as individual data points. *, Significantly different (P<0.05) from CON. CON, sham-treated leg (no light emitted). PBM, photobiomodulation treated leg.

Figure 3. Skin maximal mitochondrial respiration of the control and photobiomodulation treated leg of healthy, young adults (*n*=11). One participant was excluded due to a cytochrome C response of 17% in the PBM skin sample. Bars represent means with circles as individual data points. CON, sham-treated leg (no light emitted); PBM, photobiomodulation treated leg; JO_2, oxygen consumption rate; PM, pyruvate+malate; PMD, + adenosine diphosphate (ADP); PMDG, + glutamate; PMDGS, + succinate; PMDGSC, + cytochrome C; RCR, respiratory control ratio.

Figure 4. Muscle maximal (A) and submaximal (B) mitochondrial respiration of the control and photobiomodulation treated leg of healthy, young adults (*n*=12). Bars represent means with circles as individual data points. CON, sham-treated leg (no light emitted). PBM, photobiomodulation treated leg. JO_2, oxygen consumption rate; PM, pyruvate+malate; PMD, +

adenosine diphosphate (ADP); PMDG, + glutamate; PMDGS, + succinate; PMDGSC, + cytochrome C; RCR, respiratory control ratio.

Figure 5. Metabolic gene expression of the control and photobiomodulation treated leg of healthy, young adults (*n*=12). Gene expression of key proteins involved in the tricarboxylic acid (TCA) cycle, mitochondrial respiration, carbohydrate metabolism and fat metabolism are shown as bar graphs for CON and PBM (A, C, E, G, respectively) and as heatmaps depicting PBM as a % of the control leg for each participant, and the combined mean of the group at the bottom row (B, D, F, H, respectively). Bars represent means with circles as individual data points. *, Significantly different ($P<0.05$) from CON. CON, sham-treated leg (no light emitted). PBM, photobiomodulation treated leg.

Figure 6. Metabolic gene expression of the control and photobiomodulation treated leg of healthy, young adults (*n*=12). Gene expression of key proteins involved in oxidative stress, inflammation, cell proliferation and differentiation, heat shock proteins and endoplasmic reticulum (ER) stress are shown as bar graphs for CON and PBM (A, C, E, G, I, respectively) and as heatmaps depicting PBM as a % of the control leg for each participant, and the combined mean of the group at the bottom row (B, D, F, H, J, respectively). Bars represent means with circles as individual data points. *, Significantly different ($P<0.05$) from CON. CON, sham-treated leg (no light emitted). PBM, photobiomodulation treated leg.

SUPPLEMENTAL DIGITAL CONTENT

SDC 1: 10_Aussieker-et-al_Photobiomodulation_SDC1.docx

Figure 1

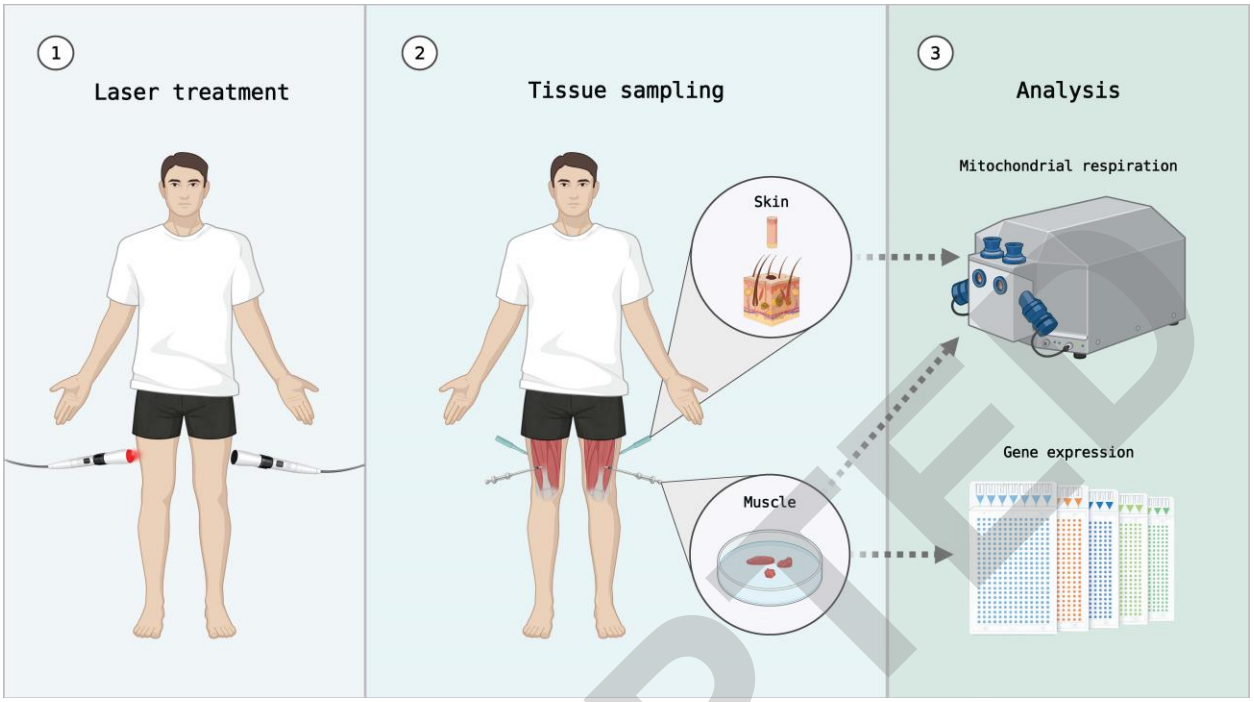

Figure 2

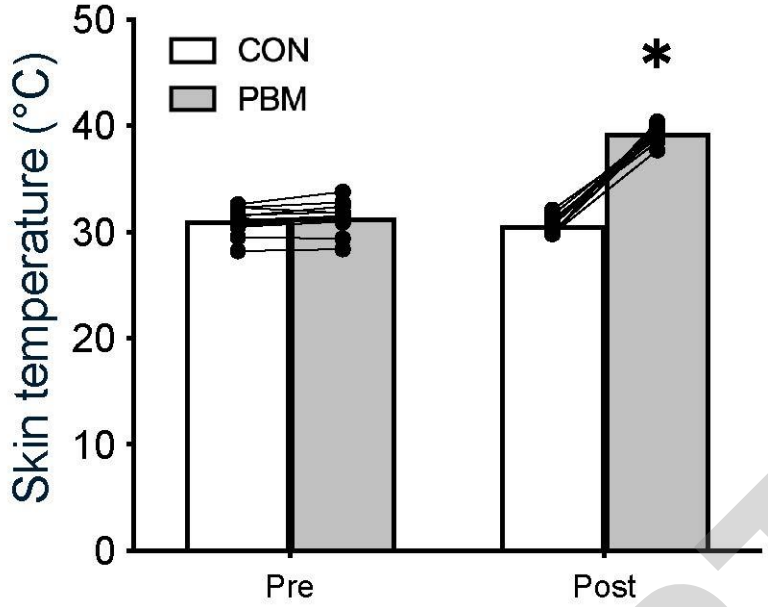

Figure 3

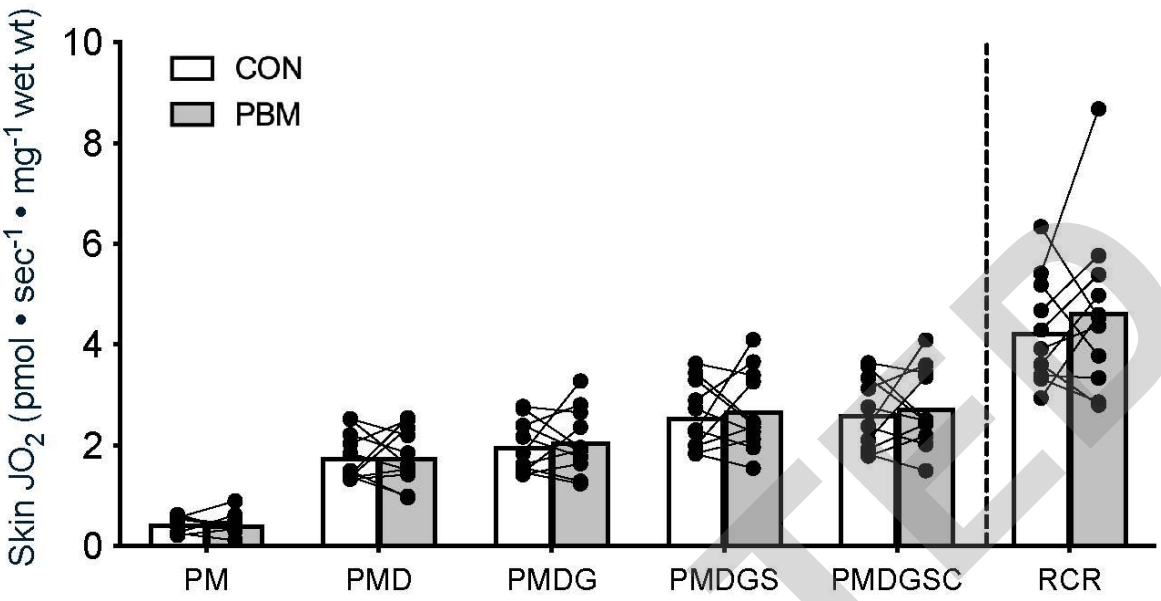

Figure 4

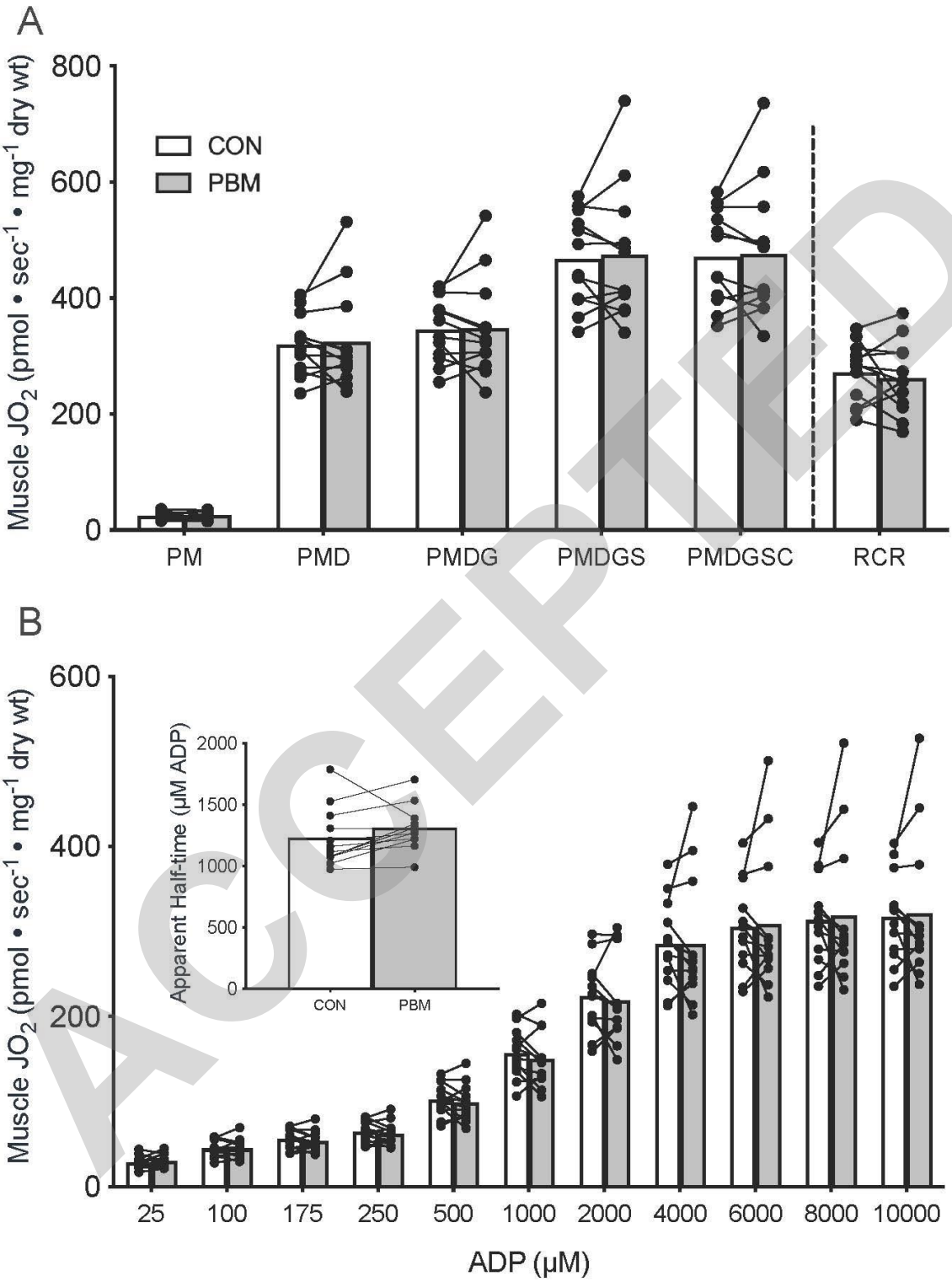

Figure 5

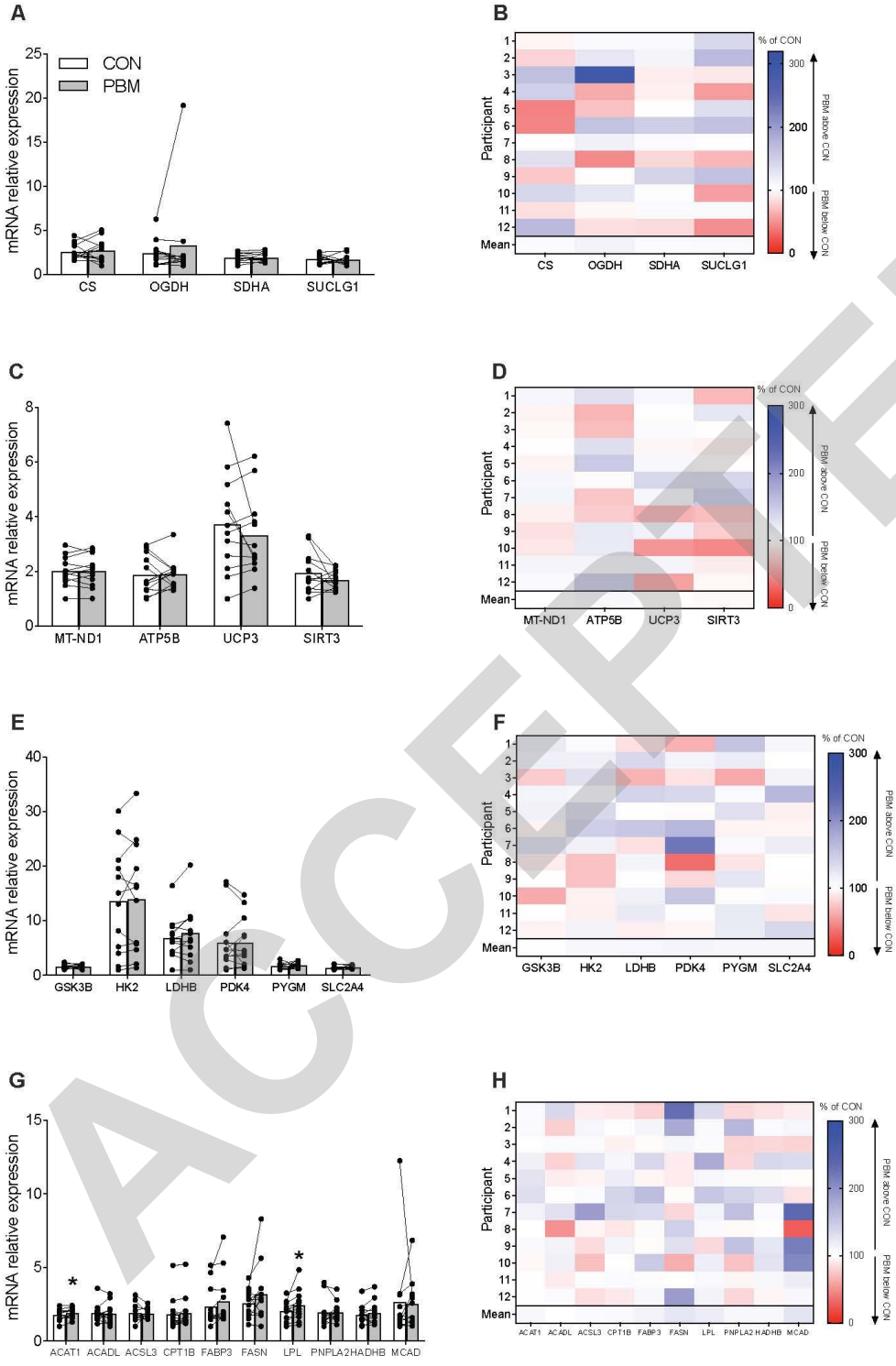

Figure 6